Nucleic Acids Research, 1997, Vol. 25, No. 24 **4899–4906**

Mirror image alternative interaction patterns of the same tRNA with either class I arginyl-tRNA synthetase or class II aspartyl-tRNA synthetase

Marie Sissler, Gilbert Eriani, Franck Martin+, Richard Giegé* and Catherine Florentz

Unité Propre de Recherche 9002 'Structure des Macromolécules Biologiques et Mécanismes de Reconnaissance', Institut de Biologie Moléculaire et Cellulaire du Centre National de la Recherche Scientifique, 15 rue René Descartes, F-67084 Strasbourg Cedex, France

Received September 11, 1997; Revised and Accepted October 27, 1997

ABSTRACT

Gene cloning, overproduction and an efficient purification protocol of yeast arginyl-tRNA synthetase (ArgRS) as well as the interaction patterns of this protein with cognate $tRNA^{Arg}$ and non-cognate $tRNA^{Asp}$ are described. This work was motivated by the fact that the *in vitro* transcript of $tRNA^{Asp}$ is of dual amino-acylation specificity and is not only aspartylated but also efficiently arginylated. The crystal structure of the complex between class II aspartyl-tRNA synthetase (AspRS) and $tRNA^{Asp}$, as well as early biochemical data, have shown that $tRNA^{Asp}$ is recognized by its variable region side. Here we show by footprinting with enzymatic and chemical probes that transcribed $tRNA^{Asp}$ is contacted by class I ArgRS along the opposite D arm side, as is homologous $tRNA^{Arg}$, but with idiosyncratic interaction patterns. Besides protection, footprints also show enhanced accessibility of the tRNAs to the structural probes, indicative of conformational changes in the complexed tRNAs. These different patterns are interpreted in relation to the alternative arginine identity sets found in the anticodon loops of $tRNA^{Arg}$ and $tRNA^{Asp}$. The mirror image alternative interaction patterns of unmodified $tRNA^{Asp}$ with either class I ArgRS or class II AspRS, accounting for the dual identity of this tRNA, are discussed in relation to the class defining features of the synthetases. This study indicates that complex formation between unmodified $tRNA^{Asp}$ and either ArgRS and AspRS is solely governed by the proteins.

INTRODUCTION

It is well established that aminoacyl-tRNA synthetases (aaRS) have to specifically interact with cognate transfer RNAs (tRNAs) in order to ensure accuracy of protein biosynthesis. Specificity of interaction is allowed thanks to nucleotide identity sets on tRNAs recognized by amino acid counterparts in homologous synthetases. A number of identity sets are already well known, in particular for all *Escherichia coli* systems and some systems of yeast and other organisms (1–3). From this knowledge it appears that identity sets are composed of a limited number of nucleotides, mostly located within the anticodon loops and the acceptor stems of the tRNAs and are unique for a given system. Footprint experiments on aaRSs on tRNAs (see for example 1,4,5) as well as knowledge of crystallographic structures of complexes (see for example 6,7) are useful to identify contacts within both molecules and in a few cases have also revealed that most of the identity elements present on the tRNA interact directly with the synthetase or, at least, contribute to an optimal conformation leading to correct positioning of the recognition elements (see for example 5,8–12).

Here we explore the interactions of yeast arginyl-tRNA synthetase (ArgRS) with its tRNA substrates. This class I synthetase is of particular interest since it is able to efficiently aminoacylate its cognate tRNA as well as a non-cognate molecule, normally specific for a class II synthetase, namely 'naked' $tRNA^{Asp}$ deprived of post-transcriptional modifications (13). This peculiarity is lost when residue G37 in the $tRNA^{Asp}$ transcript is methylated (14), a modification which occurs naturally in the mature molecule. Furthermore, previous analyses have shown that arginine identity elements are different within the $tRNA^{Arg}$ and $tRNA^{Asp}$ frameworks (15). While arginylation of yeast $tRNA^{Arg}$ is strongly related to nt C35 and to a lesser extent to U36 or G36, that of $tRNA^{Asp}$ is related to nt C36 and G37 in the anticodon loop. Mutations of these positions provoke dramatic effects on arginylation, mostly due to a decreased k_{cat}. The discovery of the two distinct identity sets was unexpected, since it was believed that such sets are unique for a given system.

Considering this functional peculiarity, it becomes important to better understand the structural features underlying the dual recognition potential of $tRNA^{Asp}$ by both class II AspRS and class I ArgRS and in the case of ArgRS to compare the non-cognate interaction pattern with the cognate one in the presence of $tRNA^{Arg}$. To investigate these tRNA–aaRS interaction features in the aspartate and arginine systems we undertook footprinting experiments of synthetases on tRNAs using several enzymatic probes as well as the phosphate-specific alkylating reagent ethylnitrosourea (ENU). These experiments revealed that ArgRS

*To whom correspondence should be addressed. Tel: +33 3 88 41 70 58; Fax: +33 3 88 60 22 18; Email: giege@ibmc.u-strasbg.fr

+Present address: Universität Bern, Zoologisches Institut, Abteilung für Entwicklungs-biologie, Baltzerstrasse 4, CH-3012 Bern, Switzerland

contacts both tRNA substrates along the same side, the D arm side, but with idiosyncratic interaction patterns, emphasizing that recognition is governed by the synthetase. Comparison with data previously obtained on the homologous AspRS–$tRNA^{Asp}$ complex highlights the topologically different interaction modes of the same tRNA by either a class I or a class II synthetase. Altogether, $tRNA^{Asp}$ is recognized by AspRS and ArgRS in a mirror image interaction scheme, as could be anticipated from comparison of the crystal structures of the glutamine and aspartate aaRS–tRNA complexes, the structural models for class I and class II complexes.

MATERIALS AND METHODS

Materials

Nucleotides, deoxynucleotides and dideoxynucleotides were from Boehringer-Mannheim (Meylan, France). The Rotiphorese Gel 40 solution of acrylamide and *N,N′*-methylene-bis-acrylamide (19:1) was from Carl Roth GmbH (Karlsruhe, Germany). Radioactive [γ-^{32}P]ATP (3000 Ci/mmol), [α-^{32}P]ATP (3000 Ci/mmol) and L-[^{3}H]arginine (57 Ci/mmol) were from Amersham (Les Ulis, France). IPTG was from GERBU (Gaiberg, Germany). Nuclease S1 and RNases T1 and V1 were from Pharmacia (Paris, France), RNase T2 from Sigma, phage T4 polynucleotide kinase from Amersham and bacterial alkaline phosphatase from Appligne (Strasbourg, France). Restriction enzymes were from New England Biolabs (Beverly, MA, USA).

Gene manipulation and enzyme purification

Yeast ArgRS was extracted from an overproducing *Escherichia coli* strain. The gene encoding ArgRS was first PCR amplified, then cloned behind the strong *Trc* promoter of plasmid pTrc99-B (16). The recipient strain TB1 (F$^-$ *ara* Δ(*lac-proAB*) *hsdR* (r_k^- m_k^+) *rpsL*(Str^r); [ϕ*80*, d*lac*Δ(*lacZ*)*M15*]) was grown to $A_{700\ nm}$ = 0.5 and then induced by adding IPTG to a final concentration of 0.5 mM. After 12 h induction cells were harvested by centrifugation and washed with TE buffer (10 mM Tris–HCl, pH 8.0, 1 mM EDTA).

Purification of the synthetase started from 35 g cells of the overproducing strain. Cells were suspended in 100 mM Tris–HCl, pH 8.0, containing 10 mM $MgCl_2$ and 1 mM EDTA and submitted to eight cycles of sonication on ice, 40 s each at 120 V (with an Annemasse Ultrasons apparatus; Annemasse, France). The supernatant obtained after 150 min centrifugation at 105 000 *g* was adsorbed on a DEAE–Sephacel column (Pharmacia Biotech, Uppsala, Sweden) equilibrated with 20 mM potassium phosphate buffer, pH 7.5, and the proteins eluted with a linear gradient of 20–400 mM buffer. Active fractions were dialyzed against 10 mM potassium phosphate buffer, pH 7.5, loaded onto a hydroxyapatite column and eluted with a linear gradient of 10–500 mM potassium phosphate, pH 7.5. The active fractions were precipitated with ammonium sulfate. The pellet was suspended in a minimal volume of 40 mM Tris–HCl, pH 7.5, loaded on a TSK HW65S column (Merck, Darmstadt, Germany) equilibrated with 40 mM Tris–HCl, pH 7.5, 2.4 M ammonium sulfate and resolved with a reverse gradient of 40 mM Tris–HCl, pH 7.5, 2.4 M ammonium sulfate to 40 mM Tris–HCl, pH 7.5. Active fractions, corresponding to pure ArgRS, were precipitated with ammonium sulfate and stored at 4°C. ArgRS activities were measured at 30°C and pH 7.5 under the reaction conditions as described previously (15).

RNA polymerase from bacteriophage T7 was purified from an overproducing strain supplied by Dr Studier (Brookhaven) according to the protocol described by Becker *et al*. (17).

Preparation of yeast $tRNA^{Asp}$ and $tRNA^{Arg}$ by *in vitro* transcription

Synthetic genes encoding for yeast $tRNA^{Asp}$ and $tRNA^{Arg}$III, downstream from the T7 RNA polymerase promoter, were constructed and cloned as previously described (15). *In vitro* transcription of these plasmids (pTFMA and pTFSMArgWT) were done after linearization as described in Frugier *et al*. (18). Transcripts were purified on 12% polyacrylamide/urea gels to single nucleotide resolution, electroeluted and ethanol precipitated. The concentration of stock solutions of transcripts were determined by absorbance measurements at $A_{260\ nm}$.

Footprinting procedures

Preparation of end-labeled RNAs. Labeling of tRNA transcripts at their 5′-end was performed with [γ-^{32}P]ATP and T4 polynucleotide kinase on molecules previously dephosphorylated with alkaline phosphatase (19). Labeling at the 3′-end resulted from [α-^{32}P]ATP exchange in the presence of (ATP, CTP):tRNA nucleotidyl transferase (G.Keith, personal communication). Labeled transcripts were purified from excess nucleotides by electrophoresis on 12% polyacrylamide gels. Bands corresponding to the labeled RNA were located on autoradiograms, excised and eluted for 2 h in 0.5 M ammonium acetate buffer, pH 6.0, containing 0.1 mM EDTA, 0.1% SDS and 10 mM magnesium acetate. After ethanol precipitation RNAs were redissolved in 10 mM HEPES–NaOH, pH 7.5, buffer containing 10 mM $MgCl_2$ and 30 mM KCl and stored at –20°C. Labeled transcripts were renaturated before any footprinting experiment by heating at 60°C for 2 min, followed by cooling to 20°C for 10 min before addition of adequate buffers and probes.

General procedures. For all footprinting experiments the final concentration of tRNA was 1 µM and that of ArgRS 8 µM. Final ArgRS concentration was such that >85% of complex is formed. Transcripts were submitted to statistical cleavage by enzymes or chemical probes followed by specific chemical cleavage of the modified positions. For enzymatic probing experiments were done on both 5′- and 3′-end labeled molecules so that distinction between primary and secondary cuts could be done (20,21). In what follows only primary cuts will be discussed. For each assay control experiments were run in parallel, without probes and in the presence or absence of ArgRS. Location of cleavage sites within the RNA structure was determined by electrophoretic separation of the RNA fragments on denaturing (8 M urea) polyacrylamide gels (12%). For assignment of cleavage positions alkaline degradations were performed in parallel by incubating the labeled RNAs for 10 min at 90°C in 50 mM $NaHCO_3$ buffer, pH 9.0. Guanine ladders were generated as described (22) by RNase T1 digestion under denaturing conditions. Signals were detected after autoradiography of the electrophoretic patterns. Quantification of the patterns was done using a Fujix Bio-Imaging Analyzer BAS 2000 system and the Work Station Software (version 1.1) for volume integration of specific cleavage sites.

Nuclease footprinting. Experiments were performed under native conditions with or without ArgRS. Digestions with the various nucleases (S1, T1, T2 and V1) were for 10 min at 30°C in 10 µl buffer (10 mM $MgCl_2$, 30 mM KCl and 10 mM HEPES–NaOH,

pH 7.5). For digestion with nuclease S1 1 mM $ZnCl_2$ was added. The reaction mixtures contained 1 µM corresponding cold tRNA species and 3′- or 5′-end-labeled transcripts (typically 50 000 Cerenkov counts). The following amounts of nucleases were added: 10^{-3} U RNase T1, 0.1 U RNase T2, 8.75×10^{-3} U RNase V1 and 25 U nuclease S1. Reactions were stopped by adding 10 µl 'stop mix' solution (0.6 M sodium acetate, pH 6.0, 3 mM EDTA and 0.1 µg/µl yeast total tRNA), followed by phenol extraction and precipitation with 200 µl 2% $LiClO_4$ in acetone (23). Pellets were washed with acetone, air dried for 10 min and redissolved in 4 M urea, 10 mM EDTA, 0.0125% xylene cyanol and 0.0125% bromophenol blue.

Phosphate alkylation with ethylnitrosourea. The method of phosphate alkylation with ENU in tRNA was essentially that already described (4,24,25). In a typical experiment ~100 000 Cerenkov counts of radioactive tRNA supplemented with the corresponding non-labeled tRNA species (~25 pmol tRNA) were incubated at 30°C for 3 h in 22.5 µl 150 mM sodium cacodylate buffer, pH 8.0, containing 10 mM $MgCl_2$ and 0.3 mM EDTA. ENU was added as a saturated ethanolic solution (2.5 µl) to 22.5 µl aqueous buffer containing both tRNA and enzyme. For all alkylation conditions controls were done in which ethanol was substituted for ethanolic ENU solution.

Alkylation reactions were stopped by adding 3 µl of 3 M sodium acetate, pH 6.0, and 2 µl non-labeled carrier tRNA. The solutions were extracted with 30 µl phenol. The tRNA was then precipitated by addition of 100 µl ethanol. After centrifugation and redissolution of the pellet in 20 µl 300 mM sodium acetate, pH 6.0, containing 20 mM EDTA, the tRNA was precipitated again with 100 µl ethanol. Modified tRNAs were split at phosphotriester positions in Tris–HCl buffer, pH 9.0 (24), and the liberated oligonucleotides analyzed by gel electrophoresis. The attention of the readers is called to the shifted migration of bands originating from 5′-labeled fragments (the presence of ethyl groups at their 3′-termini) and the numbering of electrophoretic bands (24). For other details concerning use of ENU see Romby *et al.* (4).

RESULTS AND DISCUSSION

Gene cloning, overproduction and purification of ArgRS

The gene encoding cytoplasmic yeast ArgRS (designated *RRS1*) has been located in the sequence of chromosome IV (open reading frame YDR341c of the yeast genome, ArgRS accession no. S70106; 26). Its identification was primarily based on amino acid sequences determined on tryptic peptides (27). Moreover, we identified the sequence of an internal DNA fragment which was isolated from genomic DNA by PCR amplification. According to the complete sequence yeast ArgRS is a protein of 607 residues with a calculated molecular weight of 69 524, a value in good agreement with previous experimental measurements (M_r = 73 000) (28). The protein is very similar to mitochondrial ArgRS (29) (59.5% identity, 76% similarity). Compared with *E.coli* ArgRS (30) the two enzymes display 54% identical residues and 33% similarity. Homology drops to 41% and identity to 30% when compared with the human enzyme (31).

The DNA fragment encoding *RRS1* was PCR amplified from genomic DNA starting from the first Met, where a *Nco*I site was created, to the existing *Xho*I site located 400 nt downstream of the TAA codon. The resulting DNA fragment was cloned into the multiple cloning site of pTrc99-B. This expression vector (16) is derived from pKK233-2 and carries the strong hybrid *trp*/*lac* promoter, the *lacZ* ribosome binding site, the *rrnB* transcription terminator and the *lacI*^{q} allele of the *lac* repressor gene in order to ensure complete repression of the *trp*/*lac* promoter. The ArgRS open reading frame was inserted behind the *Nco*I site of pTrc99-B, leading to a non-fused protein presenting the authentic amino acid sequence. Expression was induced by IPTG according to standard procedures (32). The whole DNA sequence was checked for PCR errors before starting enzyme purification.

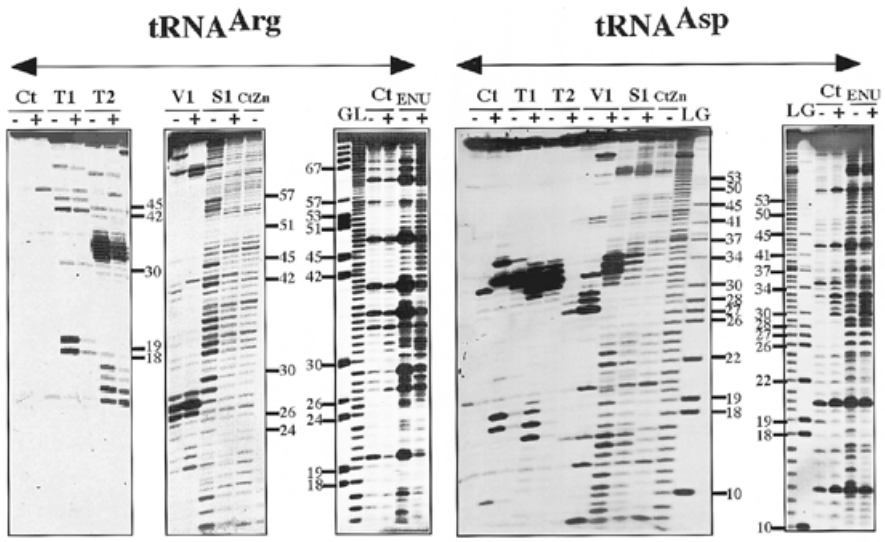

Figure 1. Autoradiograms of 12% polyacrylamide, 8 M urea gels of footprint experiments of ArgRS on 5′-labeled *in vitro* transcribed $tRNA^{Arg}$ and $tRNA^{Asp}$. Enzymatic probes (RNases T1, T2 and V1 and nuclease S1) and the chemical probe ENU were applied in the absence (–) and presence (+) of ArgRS. Control incubations performed in the absence of probes (Ct) were run in parallel. CtZn checks the effect of $ZnCl_2$ present in nuclease S1 cleavage buffer. L represents an alkaline ladder and G a denaturing RNase T1 ladder. Numbers define positions of G residues.

ArgRS purification was achieved in three chromatographic steps. About 130 mg enzyme can be recovered from an initial amount of ~35 g of cells. As judged by conventional analytic methods the protein is pure and homogeneous and has a specific activity of 4000 U/mg (1 U catalyses incorporation of 1 nmol arginine/mg enzyme/min at 30°C under aminoacylation conditions as described in 15).

Interaction of class I yeast arginyl-tRNA synthetase with its tRNA substrates

Contacts of ArgRS with *in vitro* transcribed $tRNA^{Arg}$ and $tRNA^{Asp}$ have been established by footprinting experiments using several enzymatic probes (nuclease S1 and RNases T1, T2 and V1) and one chemical reagent, ENU. Probing with the bulky S1 nuclease and RNases reveals gross features (33) such as protected single-stranded domains (with nuclease S1 and RNase T2), double-stranded or higher ordered domains (with RNase V1) or protected specific guanosines (with RNase T1). The chemical reagent ENU is a small probe and thus allows detection of specific interactions between the enzyme and phosphates from tRNAs (33,34).

Footprinting with enzymatic probes. Figure 1 presents typical autoradiograms on which RNA cleavage products obtained after treatment with the probes of ArgRS-complexed $tRNA^{Arg}$ or $tRNA^{Asp}$ are seen. For instance, with RNase T1 strong protection of residues G18 and G19 by ArgRS occurrs in both $tRNA^{Arg}$ and $tRNA^{Asp}$. Differential patterns are observed with nuclease S1 probing. For example, positions 56 and 57 are only protected in $tRNA^{Arg}$. Interestingly, footprinting revealed increased accessibilities, indicative of conformational changes in the tRNAs interacting with ArgRS. They concern in particular the 5′-part of the anticodon stem (e.g. nt 28) in RNase V1 experiments. The ensemble of data is displayed in Figure 2 on tRNA cloverleaf folds. Accessibilities of the free tRNAs to the different probes are indicated by arrowheads and protections induced by the interacting ArgRS semi-quantitatively indicated by the symbol P. Degradation sites on fragile pyrimidine/A sequences (see for example 21,35) are also indicated. Secondary cuts which are sometimes found, in particular in the anticodon arm of $tRNA^{Arg}$, are not shown.

The cleavage patterns of $tRNA^{Arg}$ and $tRNA^{Asp}$ in their free forms are consistent with the common canonical structure of

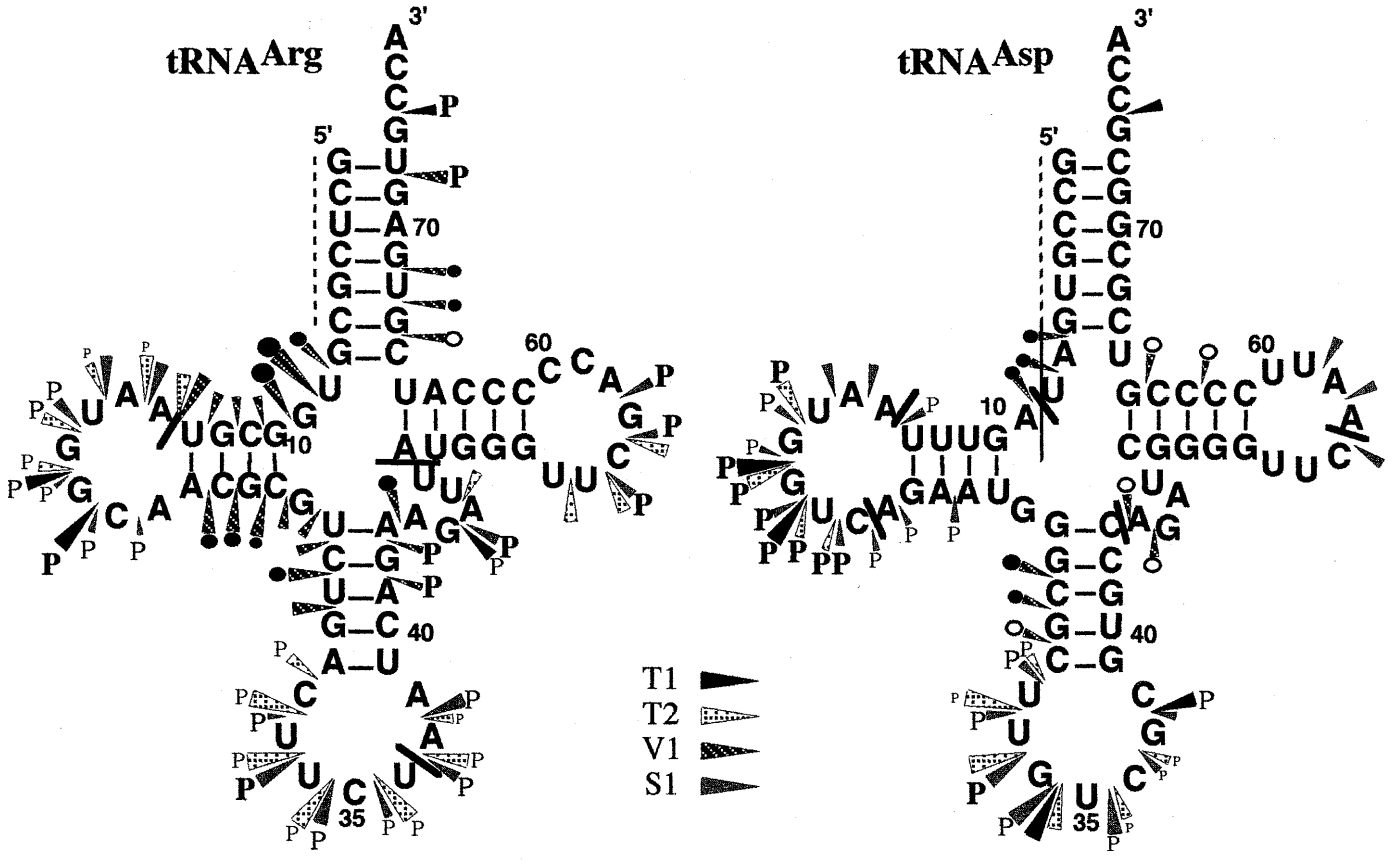

Figure 2. Footprint patterns by ArgRS on cloverleaf structures of wild-type *in vitro* transcribed yeast $tRNA^{Arg}$ and $tRNA^{Asp}$. Sequences of $tRNA^{Arg}$ and $tRNA^{Asp}$ are according to Keith and Dirheimer (53) and Gangloff *et al*. (47) respectively. Note that $tRNA^{Asp}$ transcripts possess a G1–C72 sequence as first base pair for transcription reasons. This change has no consequence on the properties of the molecule (13,48). Arrowheads correspond to positions cleaved by enzymatic probes as highlighted. Size of arrowheads is directly proportional to the intensity of cleavage, as determined by densitometry. P indicates positions where cleavage is reduced or prevented in the presence of ArgRS. Strength of protection, as determined by densitometry [weak (protection<40%), moderate (40–60%), strong (60–80%) and very strong (80–100%)], is proportional to the size of the P character. Full and open dots correspond respectively to positions where cleavage is enhanced or new in the presence of ArgRS. Strokes indicate positions of spontaneous degradation. Regions on tRNA that could not be probed are indicated (----). Note the different length of the variable region in both tRNAs (5 nt in $tRNA^{Arg}$ and 4 in $tRNA^{Asp}$) as well as that of the β domains, 3′ of the two constant G18 and G19 in their D loops (2 nt in $tRNA^{Arg}$, 3 nt in $tRNA^{Asp}$).

tRNAs. For instance, strong cuts by nuclease S1 and RNase T2 are observed within the anticodon loop and RNase V1 cuts in double-stranded regions. In the presence of ArgRS many accessibilities to the nucleases seen in the free tRNA are decreased, while a few are enhanced, thus indicating protection and conformational changes in the complexed tRNAs.

In $tRNA^{Arg}$ numerous protections occur in the D loop (nt 14–16 and 18–20), in the anticodon loop (nt 31–37) and in the T loop (nt 55–57). Additional protections are found at positions 41 and 42 in the anticodon stem, 45 in the variable loop and 71 and 73 at the acceptor stem extremity. Some cleavages in the connective region between the acceptor and D stems, in the D stem, the anticodon stem and the 3′-part of the acceptor stem are enhanced upon enzyme binding and highlight occurence of conformational changes during formation of the complex. Data presented here are in good agreement with previous results obtained with native $tRNA^{Arg}$III (36), in which RNase V1 cleavages within the anticodon and the acceptor stems were found at similar positions as in the *in vitro* transcribed tRNA. The differences, in particular in the D stem and the connective region between the acceptor and D stems, emphasize the higher plasticity of the unmodified molecule as compared with the native post-transcriptionally modified one.

As to $tRNA^{Asp}$, protections mostly occur within the D arm (nt 13, 16, 18–20, 20:1, 21 and 23) and the anticodon arm (nt 31–37). As for $tRNA^{Arg}$, several cleavages in the connective region between the acceptor and D stems, the anticodon stem, the variable region and the T stem of $tRNA^{Asp}$ are enhanced after binding of the enzyme, revealing here also the occurence of conformational changes in the tRNA during the complexation step.

It is worth mentioning the great similarities in the interaction patterns of the two tRNA molecules with ArgRS. For both the proximity sites with ArgRS are the same. However, faint differences in the patterns occur (see below).

Footprinting with ethylnitrosourea. Typical ENU experiments on $tRNA^{Arg}$ and $tRNA^{Asp}$ in the presence or absence of ArgRS are also shown in Figure 1. Quantification of ENU data is displayed in Figure 3A and a direct comparison of the interaction patterns of the two tRNAs with ArgRS is given in Figure 3B.

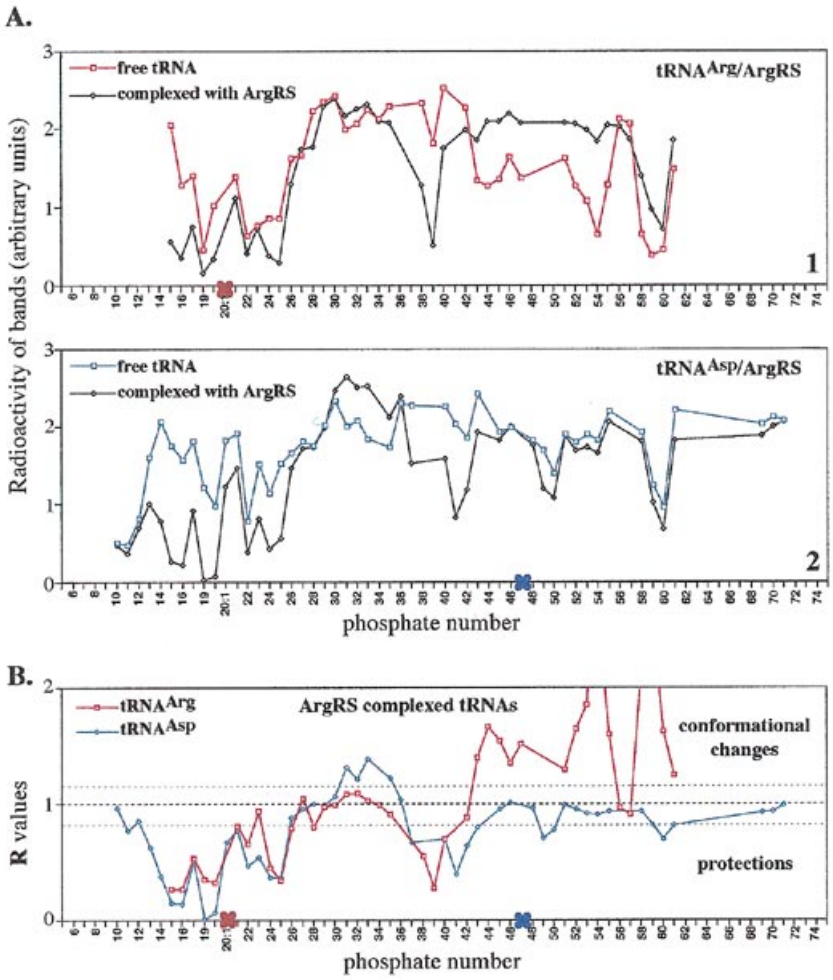

Figure 3. Analysis of the interaction areas between yeast $tRNA^{Arg}$ and $tRNA^{Asp}$ and ArgRS. (**A**) Densitometric tracings of phosphate alkylation patterns of free $tRNA^{Arg}$ (A1., red curve) and $tRNA^{Asp}$ (A2., blue curve) and of tRNAs in the presence of ArgRS (black curves). (**B**) Pattern of phosphate reactivities in tRNA transcripts complexed with ArgRS as compared with the free transcripts ($tRNA^{Arg}$/ArgRS, red; $tRNA^{Asp}$/ArgRS, blue). *R* values are ratios between intensities of electrophoretic bands corresponding to complexed and free tRNAs. Colored crosses indicate missing nucleotides in the corresponding tRNA frameworks (red for $tRNA^{Arg}$ and blue for $tRNA^{Asp}$).

Panels 1 and 2 in Figure 3A inform on accessibilities of phosphates within the free tRNAs. As already observed in many tRNAs species, phosphates of the D arm and the T loop are strongly protected against ENU alkylation. Protection of P60 reflects the particular geometry of T loops in which this phosphate interacts via two hydrogen bounds with N3C61 and the ribose 2′-OH from residue 58. An unexplained feature seen in $tRNA^{Arg}$ is protection of P54 accompanied by full reactivity of P56 and P57, up to date not observed in other tRNAs. Whether these reactivities are accounted for by the absence of modification in the T loop or are an intrinsic property of $tRNA^{Arg}$ is not yet known.

Interaction patterns of the two complexed tRNAs, as established by ENU probing, are compared in Figure 3B, with strength of protections or conformational changes quantitated by *R* values. Great similarities in the patterns of cognate $tRNA^{Arg}$ and non-cognate $tRNA^{Asp}$ occur within the 5′-part of the molecules, with strongest protections in the D (P15, 16, 18–20, 24 and 25) and anticodon arms (P38–40). Slight differences concern P23, 24 and 41, only protected in $tRNA^{Asp}$. In contrast, the two tRNAs show different enhancement patterns. Important enhancements are seen in the variable and T arm regions of ArgRS-complexed $tRNA^{Arg}$ (P44, 45, 47 and 59–61). They are not observed with non-cognate $tRNA^{Asp}$, which shows, on the contrary, slight enhancements within the anticodon arm region (P31 and 33).

Similar interaction patterns of $tRNA^{Arg}$ and $tRNA^{Asp}$ with ArgRS. All results obtained by our solution analysis are summarized on two three-dimensional models of $tRNA^{Arg}$ and $tRNA^{Asp}$ derived from the crystallographic structure of *E.coli* $tRNA^{Gln}$ as determined in the complex with GlnRS (6,37), a class I synthetase, as is ArgRS (Fig. 4). Both nuclease and ENU footprints indicate interaction of $tRNA^{Arg}$ (Fig. 4A) and $tRNA^{Asp}$ (Fig. 4B) with class I ArgRS from the D arm side (pointing towards the reader), in agreement with the interaction geometry of $tRNA^{Gln}$ with class I GlnRS as revealed by X-ray crystallography. Noteworthy are the proximities to ArgRS of the two tRNA anticodon regions, which contain the arginine identity elements previously determined in $tRNA^{Arg}$ and $tRNA^{Asp}$ (15). The figure also emphasizes the existence of great conformational changes within the complexed tRNAs. Interestingly, in both molecules the enhancements are found on the opposite side of the tRNA than that contacting the synthetase. This suggests bending of the tRNAs on the synthetase.

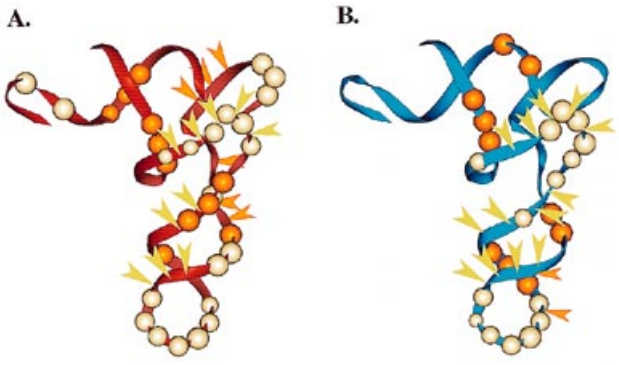

Figure 4. Three-dimensional representation of contacts between ArgRS and $tRNA^{Arg}$ (**A**) and $tRNA^{Asp}$ (**B**). The tRNAs are represented with the D arm facing forward. Light green dots highlight protection by ArgRS against enzymatic probes and orange dots enhancement of cleavage. Arrowheads with the same color code represent positions where phosphate alkylation by ENU is reduced or enhanced in the presence of ArgRS. Molecular graphic pictures were produced using the DRAWNA program (54).

Noticeable, however, are differences in the precise location of the protected tRNA regions, as well as of those undergoing conformational changes. This variability may reflect the sequence differences between the two tRNAs. However, since the probes are essentially not sequence specific, the observed variability more likely reflects intrinsic properties of the two tRNAs interacting with ArgRS. Thus the differential reactivities could arise from faint conformational changes linked to the different structural organizations of the D loops and variable regions in the two tRNAs (Fig. 2). Furthermore, we believe that this variability is a consequence of the different identity sets found in both frameworks.

Interaction of class II yeast aspartyl-tRNA synthetase with $tRNA^{Asp}$, a reminder

Aspartate tRNA aminoacylation systems are probably among the most explored, with a wealth of functional and structural data available (reviewed for example in 38–40). In the yeast system the major identity nucleotides are known (8,41) and the contacts between AspRS and $tRNA^{Asp}$ have been carefully investigated. Footprinting of the complexed tRNA by ENU gave the first clear information about tRNA contacts with the synthetase (4). They were refined when crystallography unambigously established that tRNA interacts with AspRS from its variable and T loop side and showed in addition existence of an important conformational change of the complexed tRNA (7). Furthermore, crystallography gave the precise hydrogen bonding pattern between the two interacting molecules (42). In particular, it revealed the interactions between the aspartate identity residues at the two distal ends of the tRNA and amino acids of the synthetase. Existence of these interactions was also shown by iodine probing of *in vitro* transcribed phosphorothioate-containing $tRNA^{Asp}$, which in addition revealed loss of contacts and conformational changes in tRNA mutated at identity positions (5).

For the sake of easier comparison of the aspartate and arginine systems (see below) we have represented in Figure 5 $tRNA^{Asp}$ in its non-complexed free geometry (43,44) with the location of nucleotides found in contact with AspRS highlighted in blue (left hand side of the figure). The figure illustrates well that the interacting nucleotides are on one side of the tRNA.

Yeast $tRNA^{Asp}$, a potential substrate for aminoacyl-tRNA synthetases from different classes

Figure 5 schematizes how the same tRNA, unmodified yeast $tRNA^{Asp}$, interacts efficiently either with class II AspRS (left hand side of the figure) or with the non-cognate class I ArgRS (right hand side of the figure). In the arginine case the contacts of the tRNA with ArgRS are those determined by nuclease footprinting (highlighted in yellow and green). The displayed synthetase models are sketches of the crystallographic structure of the AspRS subunit, with the catalytic domain on top and the anticodon binding domain on the bottom, and of the ArgRS overall shape derived from the known crystallographic GlnRS structure. The potential of yeast $tRNA^{Asp}$ to be recognized from both sides by two different synthetases, representative of each synthetase class, is clearly seen in the figure. Further, the geometry of tRNA–aaRS interaction in class I systems as deduced from the glutamine system can be extended to the arginine system. The

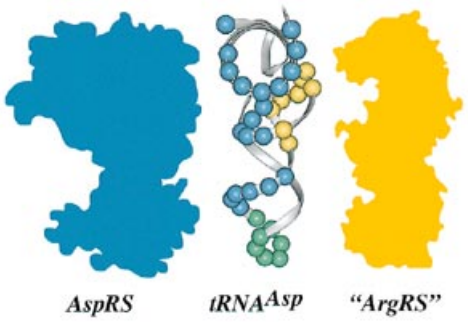

Figure 5. A 'sandwiched' interaction potential between representative class I and class II synthetases and the same tRNA substrate. Contacts in $tRNA^{Asp}$ are presented on a ribbon representation of the crystal structure of the free tRNA (43,44) with the CCA extremity pointing towards the reader. At the left hand side of the figure contacts with class II AspRS, as defined in the crystal structure of the complex (7,42), are in blue (for simplicity only one AspRS monomer is shown). At the right hand side contacts with class I ArgRS are shown in yellow (only contacts determined by enzymatic footprinting are given). Green dots correspond to common contacts with either AspRS or ArgRS. Sketches of synthetases are based on crystallographic structures of ArgRS and GlnRS in their complexed form. The synthetases are shown translated away from the tRNA for clarity. The molecular graphic picture was produced using the DRAWNA program (54).

unexpected finding is that this interaction can also occur with a tRNA normally specific for a class II synthetase. The implication is that the sequence of $tRNA^{Asp}$ without its epigenetic modifications does not contain structural features preventing its recognition by a synthetase of the other unrelated class. Thus complex formation is solely determined by the protein.

Following these lines one could hypothesize that $tRNA^{Asp}$ can be sandwiched between AspRS and ArgRS in a three component complex. This simplified view of a complex presenting two simultaneous activities, however, is unlikely for structural and mechanistic reasons. Indeed, tRNA has to undergo different types of conformational changes to specifically interact with a synthetase in a class I or class II fashion. In particular, recognition by ArgRS likely implies folding back of the CCA extremity, while with AspRS this extremity remains in helical continuity with the acceptor stem. Similarly, anticodon loops have to adopt different orientations to interact with the two enzymes. In agreement with this view are the conformational changes detected in solution in both the arginine system (this work) and the aspartate one (5).

From the functional point of view the potential of yeast $tRNA^{Asp}$ to be recognized and aminoacylated by two different yeast synthetases is biologically incompatible with specificity of protein synthesis. To encompass this drawback nature has developed a specific epigenetic strategy by introducing a structural bolt, a methyl group on G37 in $tRNA^{Asp}$, that hinders false recognition by ArgRS (14). This phenomenon is not a simple steric hindrance mechanism that would abolish interaction between $tRNA^{Asp}$ and ArgRS. Indeed, $tRNA^{Asp}$ can be complexed to ArgRS (45), but in a way allowing only poor mischarging (13,46). It follows that the negative discrimination brought about by this methyl group is the result of inefficient catalytic site activation of the synthetase by the arginine determinants contained in $tRNA^{Asp}$. The additional modified nucleosides present in native $tRNA^{Asp}$ (Ψ13, D17, D20, Ψ32, m^5C49, T54 and Ψ55; 47) likely do not participate in this negative discrimination, since the sole modification of G37 inhibits arginylation. However, a moderate role of the additional residues cannot be completely ruled out, since modifications are known to rigidify the structure of the tRNA (48) and thus would contribute to reduce its structural adaptability on ArgRS.

GENERAL CONCLUSIONS AND PERSPECTIVES

The present work demonstrates that a transcript of yeast $tRNA^{Asp}$ possessing two identity sets for specific recognition by a class I (ArgRS) and a class II (AspRS) synthetase interacts along opposite sides of its three-dimensional structure with each enzyme. It shows that the conclusions derived from our studies on the arginine system apply to class I systems of other specificities. This is actually the case for the glutamate (49), isoleucine (50) and leucine (51) systems, where ENU footprinting revealed similar interaction patterns to those reported here for tRNAs interacting with ArgRS, namely an interaction of the enzyme along the D stem of the tRNA. Occurrence of conformational changes in tRNA also seems to be a common characteristic and was clearly seen in the isoleucine system (50). Altogether, this body of solution data is in good agreement with the picture given by crystallography for the glutamine system, where both contacts along the D stem side of the tRNA and conformational changes have been observed (6). Thus this mode of interaction might be general for class I systems. Similarly, the binding mode of $tRNA^{Asp}$ with AspRS seems to be a general characteristic of class II systems and, for example, occurs in the serine system (52).

From another point of view, the possibility of a tRNA interacting with either a class I or a class II synthetase is not restricted to $tRNA^{Asp}$ and dramatic examples can be found in studies on identity permutations (for a review see for example 1). For instance, $tRNA^{Gln}$ was mutated to become an efficient substrate for class II AspRS and $tRNA^{Asp}$ to an efficient substrate for class I GlnRS (41). In that case efficient swapping of the specificities involved transplantation of identity elements and engineering of tRNA conformations. Thus different mechanisms, not only taking advantage of post-transcriptional tRNA modifications, as in the arginine/aspartate couple, but also of the chemical nature and localization of the identity residues as well as of conformational features in tRNA, are used by nature to prevent class I/class II interference.

Finally, the arginine system deserves special attention. Even if a more refined view on how yeast ArgRS can recognize either a canonical $tRNA^{Arg}$ substrate or serendipitously a $tRNA^{Asp}$ molecule has emerged from this study, a number of questions remain unsolved. In particular, one would like to understand from the structural point of view how idiosyncratic interaction patterns trigger the same arginylation reaction or, in other words, how chemical information can be conveyed from the anticodon region of tRNA to the catalytic core of the enzyme by two alternative routes. Functional and structural studies are underway to unravel these questions.

ACKNOWLEDGEMENTS

We thank Jean Gangloff and Mark Helm for fruitful discussions as well as Christian Massire for help and advice in using the program Drawna. This research was supported by grants from the Centre National de la Recherche Scientifique and Université Louis Pasteur

(Strasbourg). M.S. was supported by a MESR fellowship and F.M. by an Association pour la Recherche contre le Cancer (ARC) grant.

REFERENCES

1 Giegé,R., Puglisi,J.D. and Florentz,C. (1993) *Prog. Nucleic Acid Res. Mol. Biol*., **45**, 129–206.
2 McClain,W.H. (1993) *FASEB J*., **7**, 72–8.
3 Saks,M.E., Sampson,J.R. and Abelson,J.N. (1994) *Science*, **263**, 191–197.
4 Romby,P., Moras,D., Bergdoll,M., Dumas,P., Vlassov,V.V., Westhof,E., Ebel,J.-P. and Giegé,R. (1985) *J. Mol. Biol*., **184**, 455–471.
5 Rudinger,J., Puglisi,J.D., Pütz,J., Schatz,D., Eckstein,F., Florentz,C. and Giegé,R. (1992) *Proc. Natl. Acad. Sci. USA*, **89**, 5882–5886.
6 Rould,M.A., Perona,J.J., Söll,D. and Steitz,T.A. (1989) *Science*, **246**, 1135–1142.
7 Ruff,M., Krishnaswamy,S., Boeglin,M., Poterszman,A., Mitschler,A., Podjarny,A., Rees,B., Thierry,J.-C. and Moras,D. (1991) *Science*, **252**, 1682–1689.
8 Pütz,J., Puglisi,J.D., Florentz,C. and Giegé,R. (1991) *Science*, **252**, 1696–1699.
9 Cavarelli,J. and Moras,D. (1993) *FASEB J*., **7**, 79–86.
10 Perona,J.J., Rould,M.A. and Steitz,T.A. (1993) *Biochemistry*, **32**, 8758–8771.
11 Ibba,M., Hong,K.-W., Sherman,J.M. and Söll,D. (1996) *Proc. Natl. Acad. Sci. USA*, **93**, 6953–6958.
12 Arnez,J.G. and Steitz,T.A. (1996) *Biochemistry*, **35**, 14725–14733.
13 Perret,V., Garcia,A., Grosjean,H., Ebel,J.-P., Florentz,C. and Giegé,R. (1990) *Nature*, **344**, 787–789.
14 Pütz,J., Florentz,C., Benseler,F. and Giegé,R. (1994) *Nature Struct. Biol*., **1**, 580–582.
15 Sissler,M., Giegé,R. and Florentz,C. (1996) *EMBO J*., **15**, 5069–5076.
16 Aman,E., Ochs,B. and Abel,K.J. (1988) *Gene* **69**, 301–305.
17 Becker,H.D., Giegé,R. and Kern,D. (1996) *Biochemistry*, **35**, 7447–7458.
18 Frugier,M., Florentz,C., Schimmel,P. and Giegé,R. (1993) *Biochemistry*, **32**, 14053–14061.
19 Silberklang,F., Gillum,A.M. and RajBhandary,U.L. (1979) *Methods Enzymol*., **59**, 58–109.
20 Favorova,O.O., Fasiolo,F., Keith,G., Vassilenko,S.K. and Ebel,J.-P. (1981) *Biochemistry*, **20**, 1006–1011.
21 Florentz,C., Briand,J.-P., Romby,P., Hirth,L., Ebel,J.-P. and Giegé,R. (1982) *EMBO J*., **1**, 269–276.
22 Peattie,D.A. and Gilbert,W. (1980) *Proc. Natl. Acad. Sci. USA*, **77**, 4679–4682.
23 Vlassov,V.V., Zuber,G., Felden,B., Behr,J.-P. and Giegé,R. (1995) *Nucleic Acids Res*., **23**, 3161–3167.
24 Vlassov,V.V., Giegé,R. and Ebel,J.-P. (1981) *Eur. J. Biochem*., **119**, 51–59.
25 Vlassov,V.V., Kern,D., Romby,P., Giegé,R. and Ebel,J.-P. (1983) *Eur. J. Biochem*., **132**, 537–544.
26 Mewes,H.W., Albermann,K., Heumann,K., Liebl,S. and Pfeiffer,F. (1997) *Nucleic Acids Res*., **25**, 28–30.
27 Prévost,G. (1988). Thesis, Universit Louis Pasteur, Strasbourg.
28 Gangloff,J., Schutz,A. and Dirheimer,G. (1976) *Eur. J. Biochem*., **65**, 177–182.
29 Johnston,M. *et al*. (1994) *Science*, **265**, 2077–2082.
30 Eriani,G., Dirheimer,G. and Gangloff,J. (1989) *Nucleic Acids Res*., **17**, 5725–5735.
31 Girjes,A.A., Hobson,K., Chen,P. and Lavin,M.F. (1995) *Gene*, **164**, 347–350.
32 Ausubel,F.M., Brent,R., Kingston,R.E., Moore,D.D., Smith,J.A., Seidman,J.G. and Struhl,K. (1987) *Current Protocols in Molecular Biology*. Wiley Interscience, New York, NY.
33 Ehresmann,C., Baudin,F., Mougel,M., Romby,P., Ebel,J.-P. and Ehresmann,B. (1987) *Nucleic Acids Res*., **15**, 9109–9128.
34 Kolchanov,N.A., Titov,I.I., Vlassova,I.E. and Vlassov,V.V. (1996) *Prog. Nucleic Acid Res. Mol. Biol*., **53**, 131–197.
35 Dock-Bregeon,A.-C. and Moras,D. (1987) *Cold Spring Harbor Symp. Quant. Biol*., **52**, 113–121.
36 Gangloff,J., Jaozara,R. and Dirheimer,G. (1983) *Eur. J. Biochem*., **132**, 629–637.
37 Rould,M.A., Perona,J.J. and Steitz,T.A. (1991) *Nature*, **352**, 213–218.
38 Cavarelli,J. and Moras,D. (1995) In Söll,D. and RajBhandary,U. (eds), *tRNA: Structure, Biosynthesis, and Function*. ASM Press, Washington, DC, pp. 411–422.
39 Giegé,R., Florentz,C., Kern,D., Gangloff,J., Eriani,G. and Moras,D. (1996) *Biochimie*, **78**, 605–623.
40 Rees,B., Cavarelli,J. and Moras,D. (1996) *Biochimie*, **78**, 624–631.
41 Frugier,M., Söll,D., Giegé,R. and Florentz,C. (1994) *Biochemistry*, **33**, 9912–9921.
42 Cavarelli,J., Rees,B., Ruff,M., Thierry,J.-C. and Moras,D. (1993) *Nature*, **362**, 181–184.
43 Moras,D., Comarmond,M.B., Fischer,J., Weiss,R., Thierry,J.-C., Ebel,J.-P. and Giegé,R. (1980) *Nature*, **288**, 669–674.
44 Westhof,E., Dumas,P. and Moras,D. (1985) *J. Mol. Biol*., **184**, 119–145.
45 Gangloff,J., Ebel,J.-P. and Dirheimer,G. (1973) *Int. Res. Commun. Syst*., **12**, 8.
46 Ebel,J.-P., Giegé,R., Bonnet,J., Kern,D., Befort,N., Bollack,C., Fasiolo,F., Gangloff,J. and Dirheimer,G. (1973) *Biochimie*, **55**, 547–557.
47 Gangloff,J., Keith,G., Ebel,J.-P. and Dirheimer,G. (1971) *Nature New Biol*., **230**, 125–127.
48 Perret,V., Garcia,A., Puglisi,J.D., Grosjean,H., Ebel,J.-P., Florentz,C. and Giegé,R. (1990) *Biochimie*, **72**, 735–744.
49 Sekine,S., Nureki,O., Sakamoto,K., Niimi,T., Tateno,M., Go,M., Kohno,T., Brisson,A., Lapointe,J. and Yokoyama,S. (1996) *J. Mol. Biol*., **256**, 685–700.
50 Nureki,O., Niimi,T., Muramatsu,T., Kanno,H., Kohno,T., Florentz,C., Giegé,R. and Yokoyama,S. (1994) *J. Mol. Biol*., **236**, 710–724.
51 Dietrich,A., Romby,P., Maréchal-Drouard,L., Guillemaut,P. and Giegé,R. (1990) *Nucleic Acids Res*., **18**, 2589–2597.
52 Biou,V., Yaremchuk,A., Tukalo,M. and Cusack,S. (1994) *Science*, **263**, 1404–1410.
53 Keith,G. and Dirheimer,G. (1980) *Biochem. Biophys. Res. Commun*., **92**, 116–119.
54 Massire,C., Gaspin,C. and Westhof,E. (1994) *J. Mol. Graphics*, **12**, 201–206.